

[illegible]

# DISCLAIMER NOTICE



**THIS DOCUMENT IS BEST QUALITY AVAILABLE. THE COPY FURNISHED TO DTIC CONTAINED A SIGNIFICANT NUMBER OF PAGES WHICH DO NOT REPRODUCE LEGIBLY.**

# **A Comparison of Sources of Odd Nitrogen Production From 1974 Through 1993 in the Earth's Middle Atmosphere as Calculated Using a Two-Dimensional Model**

Francis M. Vitt

Dept. of Physics and Astronomy, University of Kansas, Lawrence

Charles H. Jackman

Laboratory for Atmospheres, NASA/Goddard Space Flight Center, Greenbelt, MD

Submitted to *Journal of Geophysical Research*, 1995

**Abstract.** The odd nitrogen source strengths associated with solar proton events (SPEs), galactic cosmic rays (GCRs), and the oxidation of nitrous oxide in the Earth's middle atmosphere from 1974 through 1993 have been compared globally, at middle and lower latitudes ( $< 50^\circ$ ), and polar regions ( $> 50^\circ$ ) with a two-dimensional (2-D) photochemical transport model. As discovered previously, the oxidation of nitrous oxide dominates the global odd nitrogen source while GCRs and SPEs are significant at polar latitudes. The horizontal transport of odd nitrogen, produced by the oxidation of nitrous oxide at latitudes  $< 50^\circ$ , was found to be the dominant source of odd nitrogen in the polar regions with GCRs contributing substantially during the entire solar cycle. The source of odd nitrogen from SPEs was more sporadic; however, contributions during several years (mostly near solar maximum) were significant in the polar middle atmosphere.

## Introduction

Odd nitrogen in the Earth's atmosphere ( $\text{NO}_y = \text{N}, \text{NO}, \text{NO}_2, \text{NO}_3, \text{N}_2\text{O}_5, \text{BrONO}_2, \text{ClONO}_2, \text{HO}_2\text{NO}_2, \text{and HNO}_3$ ) occurs only in trace amounts. Through catalytic reactions  $\text{NO}$  and  $\text{NO}_2$  act to destroy ozone in the stratosphere [Crutzen, 1970]. Consequently, the production of odd nitrogen ( $\text{NO}_y$ ) in the Earth's atmosphere has become an important consideration in the study of ozone depletion [Crutzen, 1970, 1971; Johnston, 1971; Brasseur and Nicolet, 1973; McConnell and McElroy, 1973; Crutzen et al., 1975; Johnston et al., 1979; Jackman and McPeters, 1985; Jackman et al., 1990; Reid et al., 1991; Zadorozhny et al., 1992; Jackman et al., 1993]. Odd nitrogen plays an important role in the formation of the ionospheric D region [Bates, 1952; Nicolet, 1955, 1960; Strobel et al., 1970; Strobel, 1971]. Also, odd nitrogen,  $\text{HNO}_3$  in particular, is involved in the formation of polar stratospheric clouds (PSC) which provides a mechanism for denitrification and dehydration in the colder regions of the polar stratosphere [Salawitch et al., 1989; Toon et al., 1990; Fahey et al., 1990].

The oxidation of nitrous oxide ( $\text{N}_2\text{O}$ ) is an important source of  $\text{NO}_y$  in the stratosphere. Nitrous oxide is produced by the biospheric nitrogen cycle and is transported up from the Earth's surface into the stratosphere [Bates and Hays, 1967; Nicolet and Peetermans, 1972]. Nitrous oxide reacts with  $\text{O}(^1\text{D})$ , which is produced by the photolysis of  $\text{O}_3$  in the stratosphere, to produce  $\text{NO}$ . Other sources of odd nitrogen include dissociation of  $\text{N}_2$  resulting from solar proton event (SPE) [Jackman et al., 1990] and galactic cosmic ray (GCR) interactions with the atmosphere [Nicolet, 1975]. The SPEs are the result of high energy (up to 500 MeV) solar protons originating from solar flares bombarding the middle and upper atmosphere. These events are very sporadic and vary greatly in energy spectrum. A hard event can lead to a large production of  $\text{NO}_y$  in the stratosphere at high geomagnetic latitudes. Associated with the major solar proton event of August 4, 1972, were large scale reductions in the ozone content of the middle and upper atmosphere over the polar cap regions [Heath et al., 1977;

*Reagan et al.*, 1981; *Solomon and Crutzen*, 1981; *McPeters et al.*, 1981; and *Jackman and McPeters*, 1987]. The GCRs are very high energy particles (up to a few GeV) originating from outside the solar system and are modulated by the 11 year solar cycle. These GCRs also dissociate  $N_2$  in the lower stratosphere at high geomagnetic latitudes.

In this study the SPE and GCR odd nitrogen source strengths are compared with the ambient source strength associated with nitrous oxide oxidation in various regions of the Earth's atmosphere. These odd nitrogen sources over the past twenty years (1974-1993) are evaluated using the NASA/Goddard Space Flight Center two dimensional (2-D) photochemical transport model and satellite observations of the solar particle inputs. The source strengths are compared globally, in the entire middle and low latitude region and the northern polar stratospheric region. The transport of odd nitrogen from the middle latitudes into the polar region, produced by the oxidation of nitrous oxide, is also investigated as a source strength of odd nitrogen in the northern polar stratosphere.

## Model Description

### Two-dimensional Model

The two dimensional photochemical transport model used in this study is an adaptation of the model used by *Douglass et al.* [1989] and by *Jackman et al.* [1990]. This model is zonally averaged, where the latitude range is covered by  $10^\circ$  bands centered every  $10^\circ$  ranging from  $85^\circ$  south to  $85^\circ$  north. The vertical coordinate is represented by logarithmically spaced pressure levels defined by

$$p_j = 1013 \exp[-\Delta(j - 0.5)] \text{ mb } (j = 1, 2, 3, \dots, 46) \quad (1)$$

where  $\Delta = 0.2844$ . The resulting vertical grid point separation is about 2 km, ranging approximately from the ground to approximately 90 km. The time step used is one day, photolysis reaction rates are updated every 10 days, and residual circulation

and diffusion constants are updated every 30 days. Number densities of 48 species are computed in daytime average form. Family approximations are assumed to be adequate to transport the species. Four families and twenty-one other constituents are transported.  $\text{HNO}_3$  is transported separately from  $\text{NO}_y$ . Partitioning within a chemical family is done in the fashion described by *Douglass et al.* [1989]. Temperatures used in the residual circulation calculations are based on a 4 year zonal average of National Meteorological Center (NMC) temperatures. Heating rates are taken from *Dopplick* [1974, 1979] from the ground to 100 mb, and from *Rosenfield et al.* [1987] from 100 mb to the top of the model. There are 39 wavelength intervals used in the radiative transfer scheme [Table 5 of *Douglass et al.*, 1989].

The GSFC 2-D model has been modified to incorporate a modulation of the solar photon fluxes by the 11 year solar activity cycle. The photon fluxes are modulated by use of the MgII index number published by *DeLand and Cebula* [1993] and the yearly averaged monthly sunspot number which is calculated using data from the *Solar Geophysical Data* publication. The modulation of the photon fluxes,  $\Delta\Phi$ , is calculated by using

$$\Delta\Phi(\lambda, t) = F_s(\lambda)\Delta\text{MgII}_c(t)\beta(t) \quad (2)$$

where  $F_s(\lambda)$  is the composite factor for the wavelength  $\lambda$ ,  $\Delta\text{MgII}_c$  is the amplitude of modulation in MgII index number for a given solar cycle, and  $\beta(t)$  gives the degree of modulation from the norm which is based on the yearly averaged monthly sunspot number. That is,

$$\beta(t) = \frac{N_s(t) - \langle N_s \rangle}{N_s^{\max} - \langle N_s \rangle} \quad (3)$$

where  $N_s$  is the sun spot number,  $\langle N_s \rangle = (N_s^{\min} + N_s^{\max})/2$ , and  $N_s^{\max}$  and  $N_s^{\min}$  are, respectively the maximum and minimum sun spot numbers of the corresponding solar cycle.

## NO<sub>x</sub> Production by Particle Precipitation

Atomic nitrogen is produced by SPEs and GCRs, through their primary particles or secondary electrons, causing dissociations, pre-dissociations, or dissociative ionizations in collisions with N<sub>2</sub>. We compute the atomic N or NO<sub>x</sub> (N, NO, NO<sub>2</sub>) production rate by multiplying the SPE and GCR ion pair production rate by a factor of 1.25 [Jackman *et al.*, 1980].

The ionization rate profiles produced by the GCRs at various latitudes were calculated by Nicolet [1975] at both solar maximum and solar minimum. Nicolet's results are based on the ionization rate measurements published by Neher [1967, 1971]. The rates of ionization by the GCRs for a given year are calculated using the yearly averaged monthly sunspot number of that year which is calculated using data from the *Solar Geophysical Data* publication [1993]. By linear interpolation of Nicolet's ionization rates as a function of sunspot number, ionization rates produced by the GCRs are calculated for a given year. The yearly averaged monthly sunspot number of the year 1957 corresponds to Nicolet's minimum production, while the yearly averaged monthly sunspot number of 1964 corresponds to Nicolet's maximum production. So, these sunspot numbers are used for the sunspot maximum and minimum, respectively, to calibrate the production rates from Nicolet.

A modified version of the energy deposition method of Armstrong *et al.* [1989], which uses IMP 8 (Interplanetary Monitoring Platform) particle fluxes (protons and alpha particles), is used to calculate the rates of ionization produced by the SPEs, assuming approximately 35 eV of energy is required to produce an ionization [Porter *et al.*, 1976]. The modifications include integration over pitch angle and ion pair production rate calculated versus log pressure instead of altitude. The details of this calculation are provided in the Appendix.

Figure 1 shows the evaluated energy spectrum of the proton differential fluxes using the IMP 8 daily averaged count rates of days 290 and 293 of 1989. Day 290 is during the

quiet period before the large October 1989 SPE, and day 293 is during the event. Notice that the increase in the differential flux is more than two orders of magnitude across the entire energy range and is up to three orders of magnitude at higher energies. Figure 2 illustrates the ion pair production rate before and during the October '89 event. The production rate during the event is about three orders of magnitude, or more, greater than the production rate during the quiet time before the event.

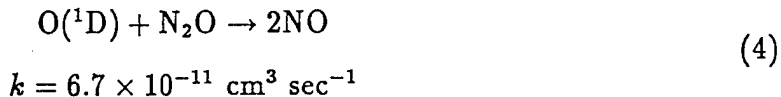
### Latitude Dependence of the Ionization by SPEs

Solar protons have virtually free access to the polar cap at geomagnetic latitudes larger than 60-65 degrees [*Reid*, 1974; *McPeters et al.*, 1981; *Reagan et al.*, 1981]. A steep gradient in a ring about five degrees in width is observed around this polar cap where the proton fluxes increase from virtually zero to their full level. We assume that the particles from the SPEs are at full strength for latitudes greater than 60 degrees geomagnetic [following *McPeters et al.*, 1981] and that the SPE flux at latitudes less than 60 degrees geomagnetic is zero. The results of the energy deposition for the polar cap (above 60° geomagnetic latitude) for the entire year of 1985 and 1989 are shown in Figure 3. Notice the substantial difference in the number of events between the two years: 1989 is near solar maximum and 1985 is near the solar minimum.

To zonally average the rates of ionization by the SPEs for the 10° geographic latitude bands centered at 85°, 75°, and 65° latitude, the geographic and geomagnetic poles are assumed to be offset by 11°. The areas where the 10° geographic and geomagnetic bands overlap are used as weighting factors of the ionization rate profiles for the corresponding geographic latitude bands.

### NO<sub>y</sub> Production Rate by O(<sup>1</sup>D) + N<sub>2</sub>O → 2NO

The production rate of odd nitrogen by the oxidation of nitrous oxide,  $P_{oz}$ ,



is calculated by using the number densities computed in the GSFC 2-D model,

$$P_{oz} = 2k[\text{O}(\text{}^1\text{D})][\text{N}_2\text{O}] \quad (5)$$

The reaction rate constant,  $k$ , is taken from the *JPL Publication 94-26* [DeMore et al., 1994]. The solar cycle ultraviolet flux changes, as described above, drive the N<sub>2</sub>O oxidation source variations over the 1974-93 time period.

### Transport of NO<sub>y</sub> into the Polar Region

Also considered as a source of odd nitrogen in the polar regions is the transport of odd nitrogen from the lower latitudes, where it is produced mainly from the oxidation of nitrous oxide. Both the advective and diffusive horizontal fluxes of the odd nitrogen are used to evaluate the number of odd nitrogen molecules transported across a vertical plane at 50° latitude. To obtain the horizontal advective flux,  $\Phi_A$ , the number density of odd nitrogen is multiplied by the meridional wind,  $v$ , used in the residual circulation of the 2-D model.

$$\Phi_A = [\text{NO}_y]v \quad (6)$$

In order to calculate the advective flux across the 50° latitude boundary for a given pressure level, the advective fluxes at the 45° and 55° grid points are averaged. The horizontal diffusive flux,  $\Phi_D$ , is determined by

$$\Phi_D = -[M]\left\{K_{yy}\frac{\partial\chi}{\partial y} + K_{yz}\frac{\partial\chi}{\partial z}\right\} \quad (7)$$

where  $K_{yy}$  and  $K_{yz}$  are the horizontal and off diagonal elements of the symmetric diffusion tensor, respectively, used in the eddy diffusion of the 2-D model, and  $\chi$  is the

mixing ratio of odd nitrogen. A central difference scheme is used to evaluate equation 7 to give the diffusive flux of odd nitrogen across the  $50^\circ$  latitude boundary for a given pressure level. The advective and diffusive fluxes are summed to give the total flux,  $\Phi_{tot}$ , i.e.,

$$\Phi_{tot} = \Phi_A + \Phi_D \quad (8)$$

$\Phi_{tot}$  is integrated over the area of the vertical plane to give the total number of odd nitrogen molecules transported into the polar region per unit time.

## Model Simulations

A steady-state calculation using the 2-D model was made without the input of ionization by the SPEs, where the model is run with fixed boundary conditions simulating the bottom boundary conditions for 1970 until a repeating annual cycle is obtained. A 4-year time dependent integration with the results of the steady-state run as the initial conditions simulated the time period from January 1, 1970, to December 31, 1973, using time dependent bottom boundary conditions. A 20-year time dependent simulation for the time period from January 1, 1974, through December 31, 1993, with the input of ionization by the SPEs was run using the results of the 4-year run as the initial conditions.

## Results

The production rate profiles are spatially averaged by integrating over latitude (meridionally averaged) in the north polar (latitudes greater than  $50^\circ$  north), middle and low latitudes (latitudes between  $50^\circ$  north and  $50^\circ$  south), and global regions. Figure 4 shows the globally averaged profiles of the SPE, GCR, and nitrous oxide oxidation sources of odd nitrogen averaged over the years 1985 and 1989. This odd nitrogen production from  $N_2O$  oxidation varies from  $3.1$  to  $3.5 \times 10^{34}$  molecules per year over

the twenty years (see Table 1). The rates of production by SPEs are about two orders of magnitude higher for 1989, near solar maximum, than for 1985, near solar minimum (varying from  $8.9 \times 10^{31}$  to  $8.4 \times 10^{33}$  molecules per year; see Table 1). The GCR source of odd nitrogen is most significant in the lower stratosphere and upper troposphere and varies from  $3.0$  to  $3.7 \times 10^{33}$  molecules per year; see Table 1. The odd nitrogen source associated with the oxidation of nitrous oxide dominates globally in the stratosphere.

By integrating the meridionally averaged profiles of the odd nitrogen production rates over the pressure coordinate, we were able to calculate the total number of  $\text{NO}_y$  molecules produced per year by the sources in the various regions of the atmosphere. Shown in Figure 5 are the total number of  $\text{NO}_y$  molecules produced globally per year calculated by integrating for the middle atmosphere above the tropopause. Figure 6 shows the total production rates in the middle and low latitude region (between  $50^\circ \text{S}$  and  $50^\circ \text{N}$ ) integrated for the middle atmosphere. In the tropics and middle latitudes, the oxidation of nitrous oxide source of odd nitrogen dominates by at least an order of magnitude over the other sources considered in this study. Figure 7 shows the odd nitrogen source strengths in the northern polar stratospheric region integrated over pressure levels between the tropopause and 1 mb and latitudes  $> 50^\circ \text{N}$  in yearly averaged form. The total source in the north polar region from the oxidation of nitrous oxide at lower latitudes transported horizontally in the stratosphere across the vertical boundary at the  $50^\circ \text{N}$  latitude is included in Figure 7. The horizontal transport source is clearly the dominant source in the polar region.

## Discussion and Conclusions

The model simulations with the input of observed proton and alpha particle fluxes indicate that the SPE source of odd nitrogen is quite sporadic and comparable to the ambient sources associated with the oxidation of nitrous oxide and GCRs at high latitudes (see Figure 7). Contrarily, the sources associated with GCRs and the oxidation

of nitrous oxide are continuous. The oxidation of nitrous oxide source varies greatly with a period of one year in the polar regions because the incident solar photon fluxes are modulated by the seasonal cycle. This source can vary by a factor of about 40 from summer to winter months. The odd nitrogen source associated with the GCRs is modulated by the 11-year solar cycle. The very active year for SPEs, 1989, produced a substantial amount of odd nitrogen in the north polar region. The SPE-produced odd nitrogen in 1989 is dominant over the GCR and ambient  $\text{N}_2\text{O} + \text{O}(^1\text{D})$  sources for that year and is about 16 % of the horizontal stratospheric transport source. The odd nitrogen horizontal transport into the polar regions from lower latitudes is also seasonally modulated. This source is positive most of the year, has its highest levels in the winter months, and can actually be negative during the summer months, when the polar region can act as a net source of odd nitrogen for the middle latitudes. In the middle and low latitudes the oxidation of nitrous oxide is the dominant source of odd nitrogen throughout the simulated period of time (see Figure 6). The GCR source is relatively constant in the middle latitudes since only the high energy galactic cosmic rays reach the lower latitudes which are influenced less by the 11 year cycle modulation.

Tables 1 and 2 give the annual source strengths for the 20-year time period in the middle atmosphere both globally and in the polar region ( $> 50^\circ$ ), respectively. The values given in Table 1 can be compared to the values of Table 2 of *Jackman et al.* [1990], hereafter referred to as J90. The  $\text{N}_2\text{O}$  oxidation source of odd nitrogen in this study (between  $3.1$  and  $3.5 \times 10^{34}$  molecules per year) is in relatively good agreement with J90 ( $\sim 2.9 \times 10^{34}$  molecules per year).

For most years, the production rates from SPEs given here are larger than those of J90. These discrepancies are primarily driven by the difference in proton spectra applied in this study compared to J90: i.e., the proton fluxes of J90 were only applied from 5 up to 100 MeV, whereas the fluxes used in this study were applicable from 0.38 MeV to 289 MeV. A second difference is that a single power law was applied over the entire

energy range in J90, whereas in this study a power law was calculated for each of the 9 proton energy ranges and 5 alpha particle energy ranges (see the Appendix). It is not clear which way this second difference in the computations will drive the odd nitrogen production values.

The production rates of odd nitrogen given in Table 1 for GCRs can be compared to those of Table 1 of *Jackman et al.* [1980]. The GCR source in this study (between  $3.0$  and  $3.7 \times 10^{33}$  molecules per year) is in relatively good agreement with *Jackman et al.* [1980] (from  $2.7$  to  $3.7 \times 10^{33}$  molecules per year).

Our study of the temporal variation of three odd nitrogen sources (SPEs, GCRs, and  $N_2O$  oxidation) of the middle atmosphere indicates  $\sim 10\%$  variations in the  $N_2O$  oxidation source,  $\sim 20\%$  variations in the GCR source, and over two orders of magnitude variations in the SPE source over a solar cycle. As shown in the previous studies [*Jackman et al.*, 1980, 1990], the  $N_2O$  oxidation source dominates the global production of odd nitrogen, when compared to the GCR and SPE sources. A new finding is the quantitative contribution of the horizontal transport of odd nitrogen, produced by the oxidation of nitrous oxide at latitudes  $< 50^\circ$ , to the polar regions. This source of odd nitrogen was found to be dominant in the polar regions during most years with GCRs contributing significantly and SPEs contributing sporadically during the solar cycle.

## Appendix: The Energy Deposition Calculation

The IMP 8 CPME (Charged Particle Measurement Experiment) daily averaged count rates are used to determine differential fluxes of both alpha particles and protons. The CPME detector of APL/JHU is aboard the IMP 8 spacecraft (also known as Explorer 50), which was launched in October of 1973 in a low inclination  $30 - 35 R_E$  orbit. A description of IMP 8 is given by *Sarris et al.* [1976]. The proton energy pass bands ranges are in Table 3. The background count rates, which are found by averaging the five lowest non-zero daily averaged count rates of each energy channel in Table 3 for

a given year, are subtracted from the daily averaged count rates.

The differential flux,  $\frac{dN}{dE}$ , is represented by assuming a power law energy dependence. That is,

$$\frac{dN}{dE} = AE^{-\gamma} \quad (A1)$$

where A is the flux constant, E is the energy of the nucleon, and  $\gamma$  is the spectral exponent.  $\frac{dN}{dE}$  and  $\gamma$  are determined from the IMP 8 daily averaged count rates, which are used to solve for A in equation A1. The flux constant, differential flux, and spectral exponent are calculated for each of the 9 proton energy ranges (5 alpha particle energy ranges) between each of the 10 proton energy passbands (6 alpha particle energy passbands) listed in Table 3. This gives usable energy ranges for the spectral exponents of 0.38 - 289 MeV and 0.82 - 37.4 MeV for the protons and alpha particles, respectively.

The integral flux for the threshold energy  $E_i$  is defined by

$$N_i^{\text{int}} = \int_{E_i}^{\infty} \frac{dN}{dE} dE \quad (A2)$$

It is also assumed here that the differential flux,  $\frac{dN}{dE}$ , has a power law energy dependence given by equation A1. Hence, the integral flux becomes

$$N_i^{\text{int}} = \frac{A}{\gamma - 1} E_i^{1-\gamma} \quad (A3)$$

The ratio of two adjacent integral fluxes, i.e.,  $N_i^{\text{int}}$  and  $N_{i+1}^{\text{int}}$ , is used to solve for  $\gamma$ . Then equation A1 is used to solve for the flux constant, A. A and  $\gamma$  are then used to give the differential flux in equation A1.

The differential fluxes are binned into small energy ranges,  $E_i$  to  $E_{i+1}$ , incident on the upper atmosphere. The integration

$$N_i = \int_{E_i}^{E_{i+1}} \frac{dN}{dE} dE \quad (A4)$$

gives the integral flux,  $N_i$ , over the energy range  $E_i$  to  $E_{i+1}$ , where  $E_i$  ( $i = 1, 2, 3, \dots, 49$  for protons and  $i = 1, 2, 3, \dots, 35$  for alpha particles) are logarithmically spaced energies

(ranging from 0.38 to 298 MeV for protons and from 0.82 to 37.4 MeV for alpha particles). The  $N_i$  can be referred to as a monoenergetic flux with an energy given by the geometric mean of the limits of integration of equation A4, i.e.,

$$E_i^0 = \sqrt{E_i E_{i+1}} \quad (\text{A5})$$

An isotropic pitch angle distribution between 0 and  $\frac{\pi}{2}$  and azimuthal symmetry are assumed. The monoenergetic fluxes have 49 discrete angles ranging from 0 to  $\frac{\pi}{2}$ , i.e., and the fluxes have incident angles  $\alpha_k^0$ , where

$$\alpha_k^0 = \sqrt{\alpha_k \alpha_{k+1}} \quad (k = 1, 2, 3, \dots, 49) \quad (\text{A6})$$

The angles,  $\alpha_k$ , are equally spaced ranging from 0 to  $\frac{\pi}{2}$ .

Now we calculate the ionization rate from the evaluated incident particle spectrum. Letting  $q_{i,j,k}$  be the rate of production of ion pairs in the  $j^{\text{th}}$  atmospheric slab by the monoenergetic flux with  $i^{\text{th}}$  incident energy at the  $k^{\text{th}}$  pitch angle, we can write

$$q_{i,j,k} = \frac{1}{35\text{eV}} \int_{\Delta\Omega_k} N_i \frac{E_{i,j,k}^D}{\Delta X_{j,k}} d\Omega \quad (\text{A7})$$

where it is assumed that on the average it takes about 35 eV [Porter *et al.*, 1976] to produce an ion pair.  $E_{i,j,k}^D$  is the energy deposited in the  $j^{\text{th}}$  slab by the flux with the  $i^{\text{th}}$  incident energy and the  $k^{\text{th}}$  pitch angle. The effective equivalent thickness of the  $j^{\text{th}}$  slab for fluxes of pitch angle  $\alpha_k^0$  is

$$\Delta X_{j,k} = \Delta Z_j \sec \alpha_k^0 \quad (\text{A8})$$

where  $\Delta Z_j$  is the actual thickness of the slab which is obtained from the GSFC 2-D model. The integration is evaluated over  $\Delta\Omega_k$ , the solid angle swept out between the angles  $\alpha_k$  and  $\alpha_{k+1}$  as the azimuthal angle is varied from 0 to  $2\pi$ .

The energy deposited in a slab of atmosphere,  $E_{i,j,k}^D$ , of equation A7 is found by using the effective equivalent thickness of the slab at STP (standard temperature and

pressure),  $X_{j,k}^{\text{STP}}$ . The effective equivalent thickness of atmospheric slab for particles of pitch angle  $\alpha_k^0$  is given by

$$\Delta X_{j,k}^{\text{STP}} = \Delta Z_j^{\text{STP}} \sec \alpha_k^0 \quad (\text{A9})$$

where  $\Delta Z_j^{\text{STP}}$  is the thickness of the  $j^{\text{th}}$  atmospheric slab at STP. The energy deposited,  $E_{i,j,k}^{\text{D}}$ , in the atmospheric slab is found by using a table look up method with the use of energy range data for protons and alpha particles in air at STP. Energy-range data for protons and alpha particles in air at STP were obtained from experimental measurements of *Bethe* [1950], *Jesse and Sadauski* [1950], *Whaling* [1958], and *Janni* [1966]. The pressure at the bottom of the  $j^{\text{th}}$  slab is given by

$$P(z_j) = \int_{z_j}^{\infty} g \rho(z) dz \quad (\text{A10})$$

where  $z_j$  is the altitude of the bottom of the  $j^{\text{th}}$  slab,  $\rho(z)$  is the mass density of the background atmosphere as a function of altitude, and  $g$  is the acceleration of gravity. Assuming that  $g$  does not change over the limits of integration, we can write the equivalent thickness,  $\Delta Z_j^{\text{STP}}$ , as

$$\Delta Z_j^{\text{STP}} = \frac{P(z_{j+1}) - P(z_j)}{g \rho_0} \quad (\text{A11})$$

where  $\rho_0$  is the atmospheric mass density at STP. Hence, we are able to calculate the equivalent slab thicknesses independent of atmospheric density profile. Pressure levels used for the energy deposition calculations are given by equation 1, here  $j = 1, 2, \dots, 60$ .

Assuming that the fluxes, energy deposited, and effective equivalent thicknesses do not change significantly as the pitch angle varies over the integration limits in equation A7, we can write

$$q_{i,j,k} = \frac{1}{35\text{eV}} N_i \frac{E_{i,j,k}^{\text{D}}}{\Delta Z_j} 2\pi (\cos \alpha_{k+1} - \cos \alpha_k) \cos \alpha_k^0 \quad (\text{A12})$$

This is the ion pair production rate in the  $j^{\text{th}}$  slab, or  $j^{\text{th}}$  pressure level, produced by the monoenergetic flux with the  $i^{\text{th}}$  incident energy and  $k^{\text{th}}$  pitch angle. Summing

over incident pitch angles and incident energies, we can calculate the total ion pair production rate in the  $j^{\text{th}}$  slab.

The energy conservation is also checked in the energy computation. The calculation of the total energy entering the top of the atmosphere, when integrating over the energy spectrum, has been found to be equal to the total energy deposited in the atmosphere.

### Acknowledgments

Support for the research is provided by Air Force grant AFOSR 88-0065 and ASSERT F49620 - 92 - J - 0235DEF. Advice and consultation with Prof. T. E. Cravens, Prof. T. P. Armstrong, and Dr. G. Dreschhoff were helpful. Acknowledgment is made for the use of the IMP 8 proton and alpha particle fluxes.

## References

- Armstrong, T. P., C. M. Laird, D. Venkatesan, S. Krishnaswamy, and T. J. Rosenberg, Interplanetary energetic ions and polar radio wave absorption, *J. Geophys. Res.*, **94**, 3543-3554, 1989.
- Bates, D. R., Some reactions occurring in the Earth's upper atmosphere, *Ann. Geophys.*, **8**, 194 - 204, 1952.
- Bates, D. R., and P. B. Hays, Atmospheric nitrous oxide, *Planet. Space Sci.*, **15**, 189-197, 1967.
- Bethe, H. A., The range-energy relation for slow alpha-particles and protons in air, *Rev. Mod. Phys.*, **22**, 213-219, 1950.
- Brasseur, G., and M. Nicolet, Chemical processes of nitric oxide in the mesosphere and stratosphere, *Planet. Space Sci.*, **21**, 939-961, 1973.
- Crutzen, P. J., The influence of nitrogen oxides on the atmospheric ozone content, *Quart. J. Roy. Meteorol. Soc.*, **96**, 320-325, 1970.
- Crutzen, P. J., Ozone production rates in an oxygen-hydrogen-nitrogen oxide atmosphere, *J. Geophys. Res.*, **76**, 7311-7327, 1971.
- Crutzen, P. J., I. S. A. Isaksen, and G. C. Reid, Solar proton events: stratospheric source of nitric oxide, *Science*, **189**, 457-459, 1975.
- DeLand, Matthew T., and Richard P. Cebula, Composite MG II solar activity index for solar cycles 21 and 22, *J. Geophys. Res.*, **98**, 12809-12823, 1993.
- DeMore, W. B., S. P. Sander, D. M. Golden, R. F. Hampson, M. J. Kurylo, C. J. Howard, A. R. Ravishankara, C. E. Kolb, and M. J. Molina, *Chemical Kinetics and Photochemical Data for Use in Stratospheric Modeling, Evaluation No. 11*, JPL Publication 94-26, NASA/JPL, Pasadena, CA, 1994.

- Dopplick, T. G., The heat budget, in *The General Circulation of the Tropical Atmosphere and Interactions With Extratropical Latitudes*, vol. 2, chap. 7, edited by R. E. Newell, J. W. Kidson, D. G. Vincent, and C. J. Boer, The MIT Press, Cambridge, Mass., 1974.
- Dopplick, T. G., Radiative heating of the global atmosphere: Corrigendum, *J. Atmos. Sci.*, *36*, 1812-1817, 1979.
- Douglass, A. R., C. H. Jackman, and R. S. Stolarski, Comparison of model results transporting the odd nitrogen family with results transporting separate odd nitrogen species, *J. Geophys. Res.*, *94*, 9862-9872, 1989.
- Fahey, D. W., K. K. Kelly, S. R. Kawa, A. F. Tuck, M. Loewenstien, K. R. Chan, and L. E. Heidt, Observations of denitrification and dehydration in the winter polar stratospheres, *Nature*, *344*, 321-324, 1990.
- Heath, Donald F., A. J. Krueger, and P. J. Crutzen, Solar proton event: influence of stratospheric ozone, *Science*, *197*, 886-888, 1977.
- Jackman, C. H., J. E. Frederick, and R. S. Stolarski, Production of odd nitrogen in the stratosphere and mesosphere: An intercomparison of source strengths, *J. Geophys. Res.*, *85*, 7495-7505, 1980.
- Jackman, C. H., and R. D. McPeters, The response of ozone to solar proton events during solar cycle 21: a theoretical interpretation, *J. Geophys. Res.*, *90*, 7955-7966, 1985.
- Jackman, C. H., and R. D. McPeters, Solar proton events as tests for the fidelity of middle atmosphere models, *Physica Scripta*, *T18*, 309-316, 1987.
- Jackman, C. H., A. R. Douglass, R. B. Rood, and R. D. McPeters, Effect of solar proton events on the middle atmosphere during the past two solar cycles as computed using a two-dimensional model, *J. Geophys. Res.*, *95*, 7417-7428, 1990.

- Jackman, C. H., J. E. Nielsen, D. J. Allen, M. C. Cerniglia, R. D. McPeters, A. R. Douglass, and R. B. Rood, The effects of the October 1989 solar proton events on the stratosphere as computed using a three dimensional model, *Geophys. Res. Lett.*, *20*, 459-462, 1993.
- Janni, Calculations of energy loss, range, path length, etc., *Tech. Rep. AFWL-TR-65-150*, pp 318, U. S. Air Force Base, Kirtland Airforce Base, N. M., 1966.
- Jesse, J. P., and J. Sadauski, The range-energy curves for alpha particles and protons, *Phys. Rev.*, *78*, 1-8, 1950.
- Johnston, H. S., Reduction of stratospheric ozone by nitrogen oxide catalysts from supersonic transport exhaust, *Science*, *173*, 517-522, 1971
- Johnston, H. S., O. Serang, and J. Podolske, Instantaneous global nitrous oxide photochemical rates, *J. Geophys. Res.*, *84*, 5077-5082, 1979.
- McConnell, J. C., and M. B. McElroy, Odd nitrogen in the atmosphere, *J. Atmos. Sci.*, *31*, 1465-1486, 1973.
- McPeters, R. D., C. H. Jackman, and E. G. Stassinopoulos, Observations of ozone depletion associated with solar proton events, *J. Geophys. Res.*, *86*, 12071-12081, 1981.
- National Geophysical Data Center, *Solar Geophysical Data, No. 585-Part I*, 1993.
- Neher, H. V., Cosmic-ray particles that changed from 1954 to 1958 to 1965, *J. Geophys. Res.*, *72*, 1527-1539, 1967.
- Neher, H. V., Cosmic rays at high latitudes and altitudes covering four solar maxima, *J. Geophys. Res.*, *76*, 1637-1651, 1971.
- Nicolet, M., Nitrogen oxides and the airglow, *J. Atmos. Terr. Phys.*, *7*, 297-309, 1955.
- Nicolet, M., Aeronomic chemical reactions, in *The Physics and Medicine of the Atmosphere and Space*, edited by O. D. Benson, Jr. and H. Strughold, pp 14-47, John Wiley, New York, 1960.

- Nicolet, M., On the production of nitric oxide by cosmic rays in the mesosphere and stratosphere, *Planet. Space Sci.*, **23**, 637-649, 1975.
- Nicolet, M., and W. Peetermans, The production of nitric oxide in the stratosphere by oxidation of nitrous oxide, *Ann. Geophys.*, **28**, 751-761, 1972.
- Porter, H. S., C. H. Jackman, and A. E. S. Green, Efficiencies for production of atomic nitrogen and oxygen by relativistic proton impact in air, *J. Chem. Phys.*, **65**, 154-167, 1976.
- Reagan, J. B., R. E. Meyerott, R. W. Nightingale, R. C. Gunton, R. G. Johnson, J. E. Evans, W. L. Imhof, D. F. Heath, and A. J. Krueger, Effects of the August 1972 solar particle events on stratospheric ozone, *J. Geophys. Res.*, **86**, 1473-1494, 1981.
- Reid, G. C., Polar-cap absorption - Observations and theory, *Fundamentals of Cosmic Physics*, **1**, 167-200, 1974.
- Reid, G. C., S. Solomon, and R. R. Garcia, Response of the middle atmosphere to the solar proton events of August - December, *Geophys. Res. Lett.*, **18**, 1019-1022, 1991.
- Rosenfield, J. E., M. R. Schoeberl, and M. A. Geller, A computation of the stratospheric diabatic residual circulation using an accurate radiative transfer model, *J. Atmos. Sci.*, **44**, 859-876, 1987.
- Salawitch, R. J., G. P. Gobbi, S. C. Wofsy, and M. B. McElroy, Denitrification in the Antarctic stratosphere, *Nature*, **339**, 525-527, 1989.
- Sarris, E. T., S. M. Krimigis, and T. P. Armstrong, Observations of magnetospheric bursts of high-energy protons and electrons at 35  $R_E$  with IMP 7, *J. Geophys. Res.*, **81**, 2341-2355, 1976.
- Solomon, S., and P. J. Crutzen, Analysis of the 1972 solar proton event including chlorine chemistry, *J. Geophys. Res.*, **86**, 1140-1146, 1981.
- Strobel, D. F., Odd nitrogen in the mesosphere, *J. Geophys. Res.*, **76**, 8384-8393, 1971.

- Strobel, D. F., D. M. Hunten, and M. B. McElroy, Production and diffusion of nitric oxide, *J. Geophys. Res.*, *75*, 4307-4321, 1970.
- Toon, O. B., R. P. Turco, and P. Hamill, Denitrification mechanisms in the polar stratosphere, *Geophys. Res. Lett.*, *17*, 445-448, 1990.
- Whaling, W., The energy loss of charged particles in matter, *Handb. Phys.*, *34*, 193, 1958.
- Zadorozhny, A. M., G. A. Tuchkov, V. N. Kikhtendo, J. Lastovicka, J. Boska, and A. Novak, Nitric oxide and lower ionosphere quantities during solar particle events of October 1989 after rocket and ground-based measurements, *J. Atmos. Terr. Phys.*, *54*, 183 - 192, 1992.

## Figures

**Figure 1.** The energy spectrum of the differential proton fluxes evaluated by use of the daily averaged proton count rates measured by IMP 8. Day 290 is before and day 293 is during the very large solar particle event which occurred in October of '89.

**Figure 2.** The rate of ion pair production evaluated using IMP 8 daily averaged count rates of protons and alpha particles which are input into an energy deposition calculation. Day 290 is before and day 293 is during the very large solar particle event which occurred in October of '89.

**Figure 3.** Logarithm (base 10) of the rate of ionization in the polar region versus pressure versus time for the entire year of 1985 and 1989 evaluated using daily averaged count rates of protons and alpha particles measured by IMP 8. 1985 is near solar minimum and 1989 is near solar maximum.

Figure 4. The yearly and globally averaged rate of odd nitrogen production profiles for a near solar minimum year, 1985, and a near solar maximum year, 1989.

Figure 5. The total number of odd nitrogen molecules produced globally per year in the middle atmosphere by SPEs, GCRs, and the oxidation of nitrous oxide.

Figure 6. The total number of odd nitrogen molecules produced per year by SPEs, GCRs, and oxidation of nitrous oxide in the middle atmosphere in the region between 50° north and 50° south latitudes.

Figure 7. The total number of odd nitrogen molecules produced per year by SPEs, GCRs, and oxidation of nitrous oxide sources in the north polar stratosphere, latitudes > 50° N and pressure levels between the tropopause and 1 mb.

**Table 1.** Odd nitrogen molecules computed to be produced per year globally in the middle atmosphere by solar proton events (SPEs), galactic cosmic rays (GCRs), and the oxidation of  $\text{N}_2\text{O}$ .

Year	SPE Meso.	SPE Strato.	SPE Total	GCR Strat.	$\text{N}_2\text{O} + \text{O}(^1\text{D})$ Strat.
1974	3.6(32)	5.2(31)	4.1(32)	3.6(33)	3.2(34)
1975	4.5(30)	8.5(30)	1.3(31)	3.7(33)	3.2(34)
1976	2.1(31)	2.8(31)	4.9(31)	3.7(33)	3.3(34)
1977	1.6(32)	7.2(31)	2.4(32)	3.6(33)	3.3(34)
1978	1.9(33)	3.5(32)	2.2(33)	3.3(33)	3.3(34)
1979	5.9(32)	1.3(32)	7.3(32)	3.0(33)	3.3(34)
1980	1.8(32)	1.9(31)	2.0(32)	3.0(33)	3.2(34)
1981	1.5(33)	2.6(32)	1.7(33)	3.0(33)	3.1(34)
1982	1.2(33)	2.1(32)	1.4(33)	3.2(33)	3.2(34)
1983	1.9(32)	1.4(31)	2.0(32)	3.4(33)	3.2(34)
1984	5.4(32)	2.9(32)	8.3(32)	3.5(33)	3.3(34)
1985	7.4(31)	1.5(31)	8.9(31)	3.7(33)	3.4(34)
1986	1.6(32)	4.7(31)	2.1(32)	3.7(33)	3.4(34)
1987	2.1(31)	9.0(30)	3.0(31)	3.6(33)	3.5(34)
1988	1.4(32)	1.8(31)	1.5(32)	3.2(33)	3.5(34)
1989	5.1(33)	3.3(33)	8.4(33)	3.0(33)	3.4(34)
1990	5.1(32)	1.2(32)	6.2(32)	3.0(33)	3.3(34)
1991	2.0(33)	5.4(32)	2.5(33)	3.0(33)	3.3(34)
1992	9.7(32)	2.6(32)	1.2(33)	3.3(33)	3.3(34)
1993	4.2(31)	1.1(32)	1.5(32)	3.4(33)	3.4(34)

**Table 2.** Odd nitrogen molecules produced per year in the north polar region ( $> 50^\circ \text{ N}$ ) in the middle atmosphere by solar proton events (SPEs), galactic cosmic rays (GCRs), the oxidation of  $\text{N}_2\text{O}$ , and the horizontal transport of odd nitrogen into the polar region produced by  $\text{N}_2\text{O} + \text{O}(^1\text{D})$  in middle and lower latitudes.

Year	SPE Meso.	SPE Strat.	SPE Total	GCR Strat.	$\text{N}_2\text{O} + \text{O}(^1\text{D})$ Strat.	Hor. Trans. of Odd N in Strat.
1974	1.8(32)	2.6(31)	2.1(32)	9.2(32)	9.79(32)	8.65(33)
1975	2.3(30)	4.2(30)	6.5(30)	9.6(32)	9.86(32)	9.11(33)
1976	1.1(31)	1.4(31)	2.4(31)	9.6(32)	1.00(33)	9.27(33)
1977	8.1(31)	3.6(31)	1.2(32)	9.4(32)	1.01(33)	9.42(33)
1978	9.3(32)	1.7(32)	1.1(33)	8.1(32)	1.02(33)	9.54(33)
1979	2.9(32)	6.6(31)	3.6(32)	7.0(32)	9.87(32)	9.52(33)
1980	9.1(31)	9.4(30)	1.0(32)	7.0(32)	9.49(32)	9.20(33)
1981	7.3(32)	1.3(32)	8.6(32)	7.3(32)	9.41(32)	8.75(33)
1982	5.7(32)	1.0(32)	6.8(32)	7.7(32)	9.51(32)	8.54(33)
1983	9.4(31)	7.1(30)	1.0(32)	8.6(32)	9.69(32)	8.56(33)
1984	2.7(32)	1.5(32)	4.1(32)	9.0(32)	1.00(33)	8.73(33)
1985	3.7(31)	7.7(30)	4.4(31)	9.5(32)	1.03(33)	9.06(33)
1986	7.9(31)	2.3(31)	1.0(32)	9.6(32)	1.05(33)	9.39(33)
1987	1.0(31)	4.5(30)	1.5(31)	9.3(32)	1.07(33)	9.70(33)
1988	6.7(31)	8.8(30)	7.6(31)	8.0(32)	1.07(33)	9.92(33)
1989	2.5(33)	1.6(33)	4.2(33)	6.9(32)	1.04(33)	9.97(33)
1990	2.5(32)	5.8(31)	3.1(32)	7.2(32)	1.01(33)	9.63(33)
1991	9.8(32)	2.7(32)	1.3(33)	7.2(32)	1.00(33)	9.14(33)
1992	4.8(32)	1.3(32)	6.1(32)	8.1(32)	1.00(33)	8.96(33)
1993	2.1(31)	5.3(31)	7.4(31)	8.5(32)	1.03(33)	8.98(33)

**Table 3.** The IMP 8 CPME passband energy ranges.

Channel	Passband	Species
P1	0.29 - 0.50 MeV	Protons
P2	0.50 - 0.96 MeV	Protons
P3	0.96 - 2.00 MeV	Protons
P4	2.00 - 4.60 MeV	Protons
P5	4.60 - 15.0 MeV	Protons
P7	15.0 - 25.0 MeV	Protons
P8	25.0 - 48.0 MeV	Protons
P9	48.0 - 96.0 MeV	Protons
P10	96.0 - 145 MeV	Protons
P11	190 - 440 MeV	Protons
A1	0.59 - 1.14 MeV	Alpha Particles
A2	1.14 - 1.80 MeV	Alpha Particles
A3	1.80 - 4.20 MeV	Alpha Particles
A4	4.20 - 12.0 MeV	Alpha Particles
A5	12.0 - 28.0 MeV	Alpha Particles
A6	28.0 - 52.0 MeV	Alpha Particles

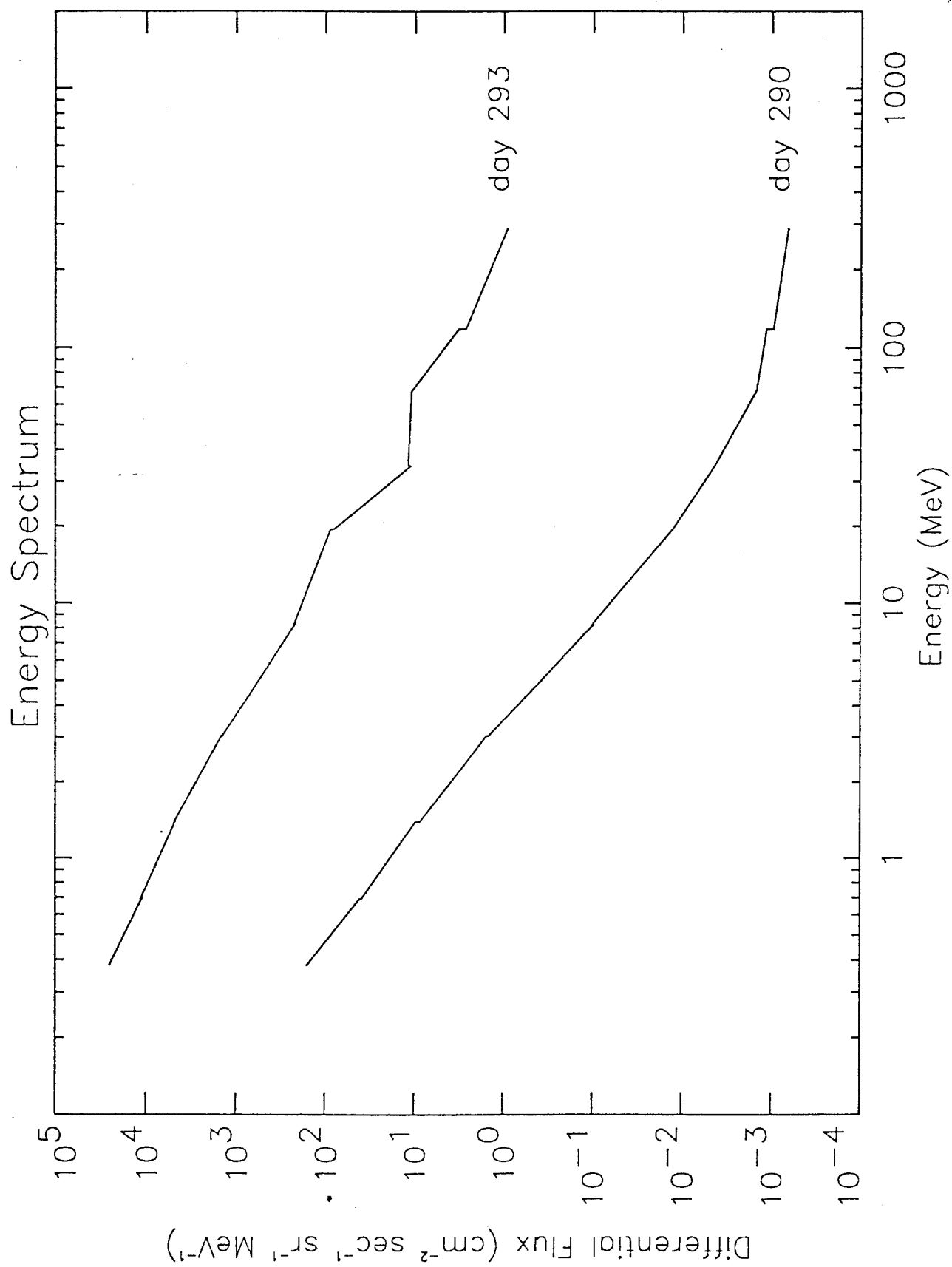


Figure 1

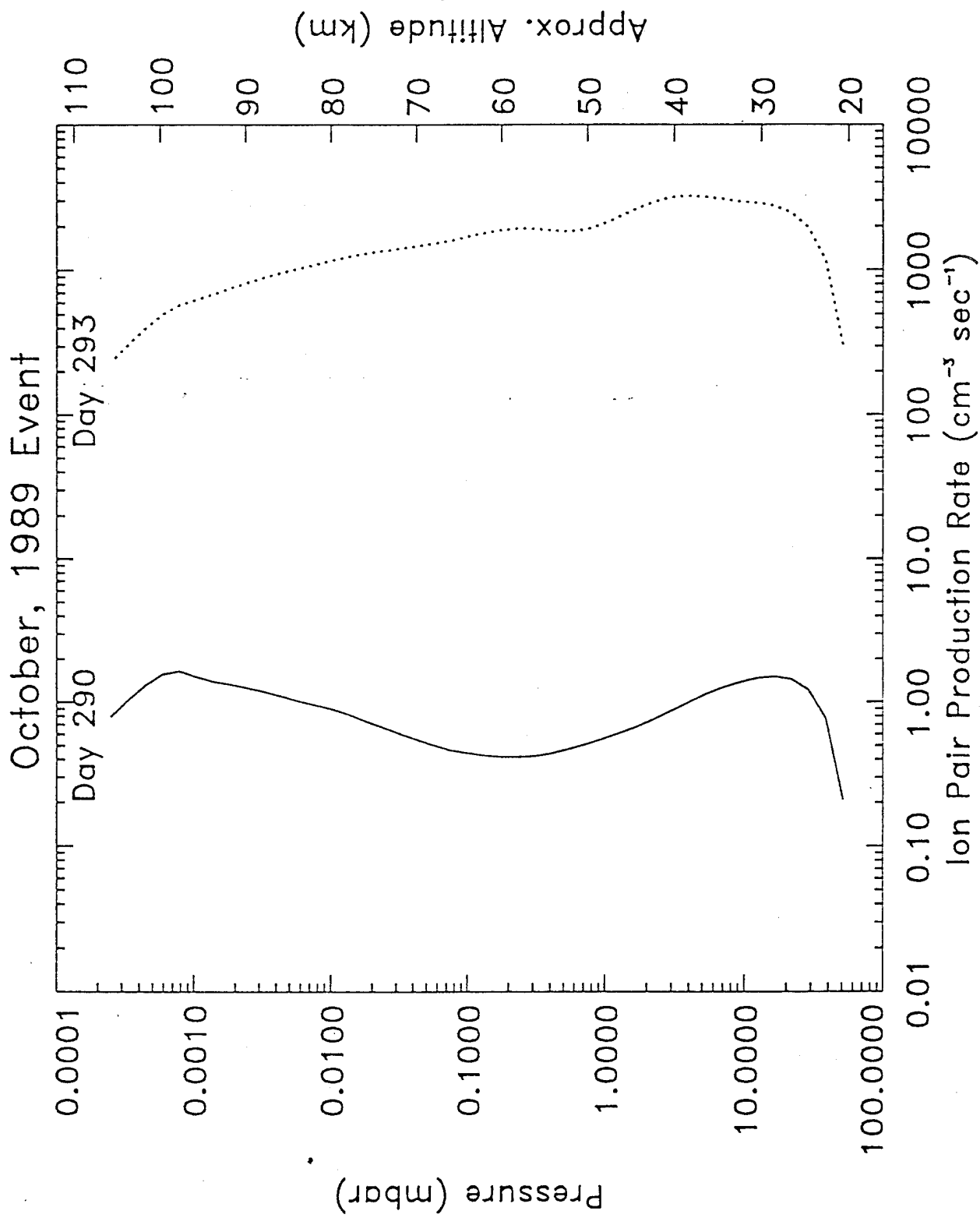


Figure 2

# Ionization by SPEs in the Polar Region

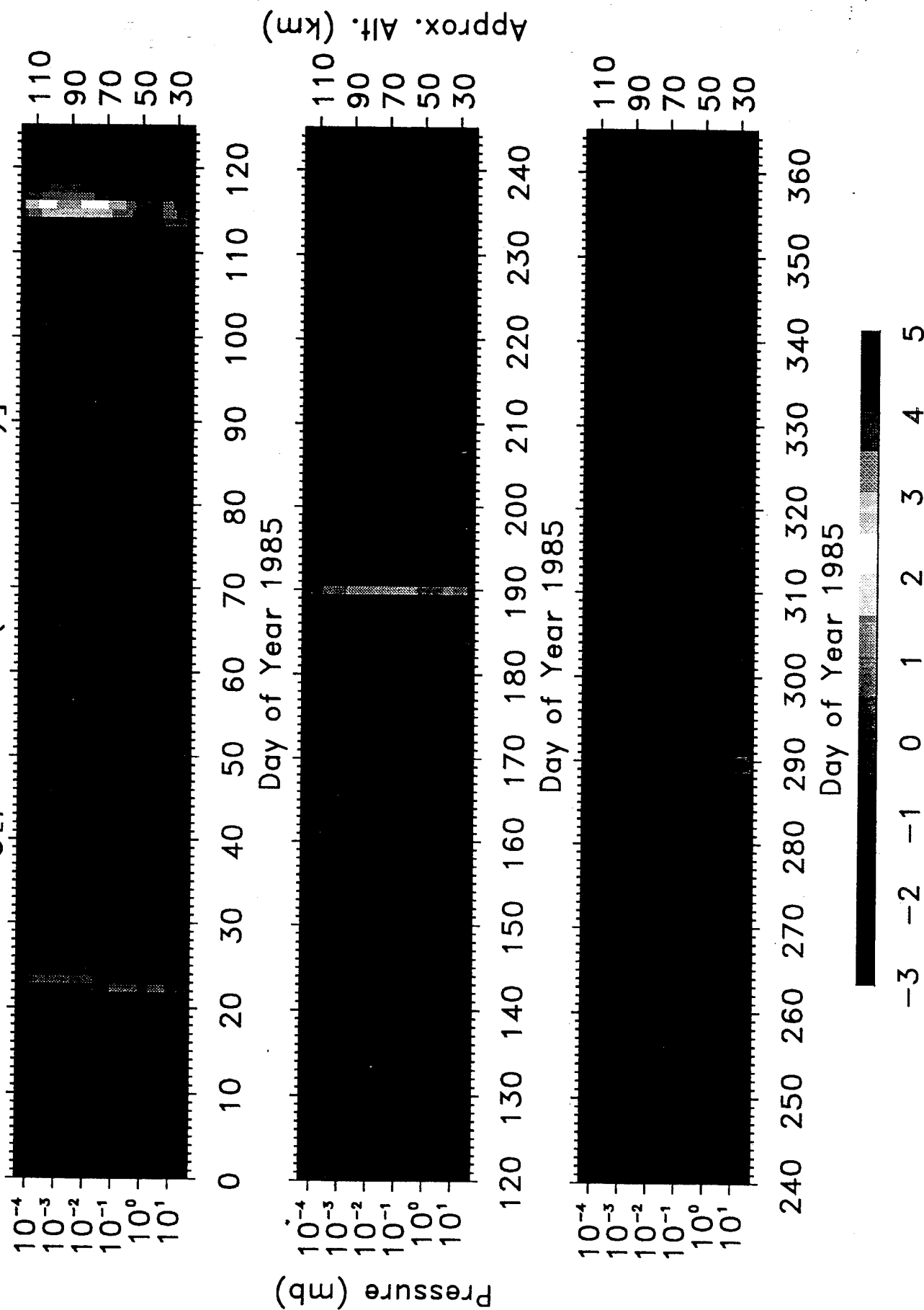


Fig. 3a

# Ionization by SPEs in the Polar Region

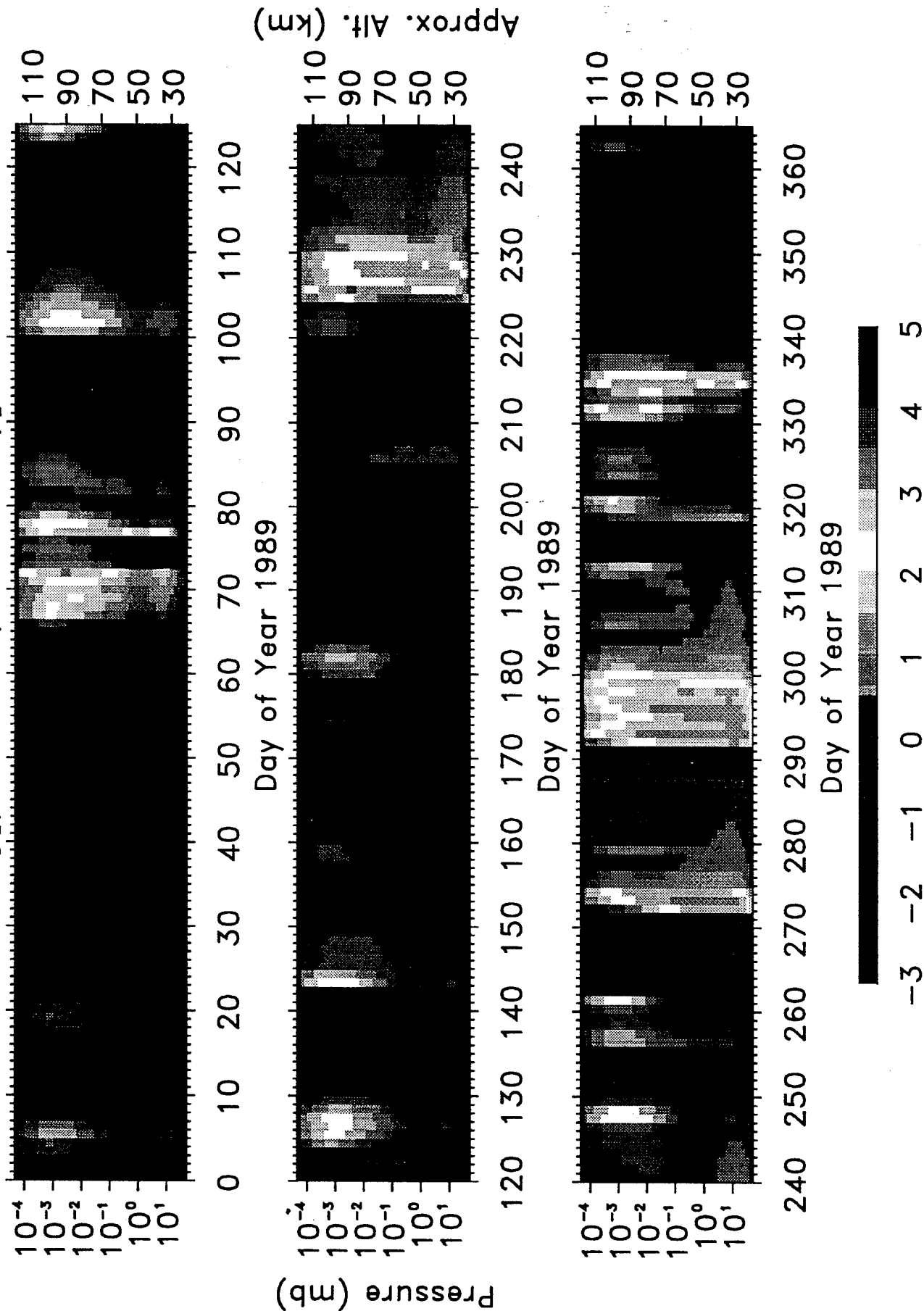


Fig. 3b

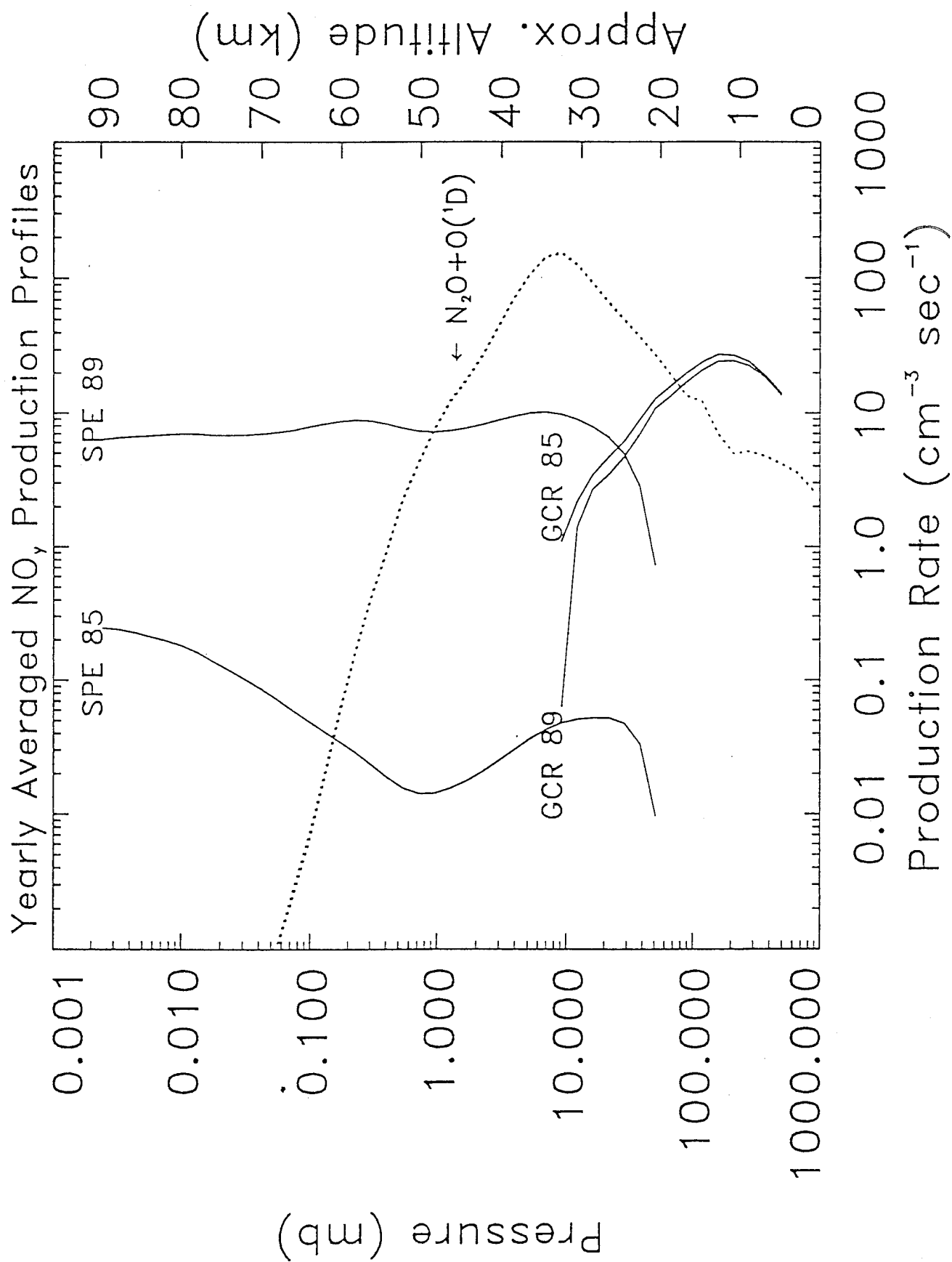


Figure 4

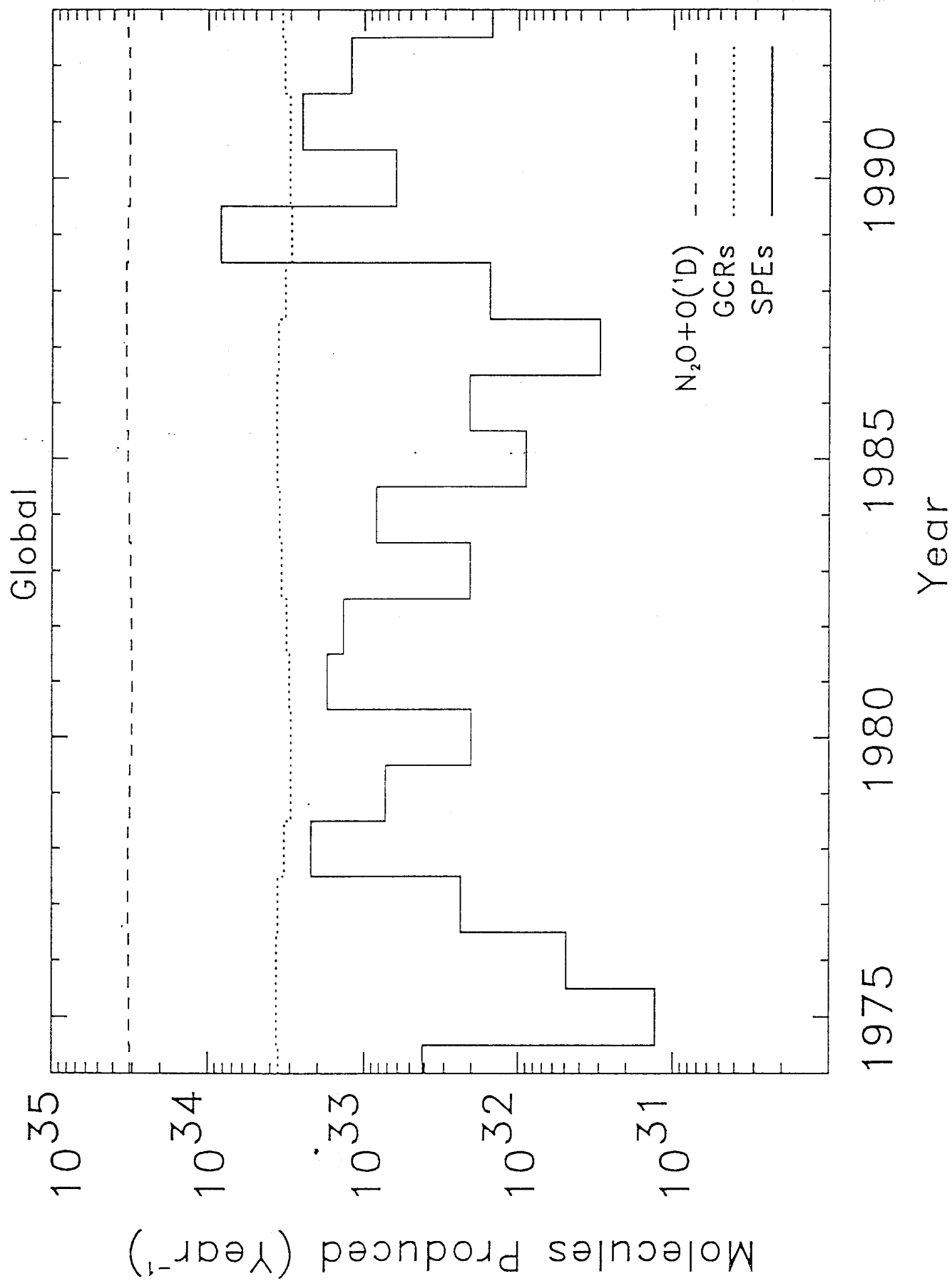


Figure 5

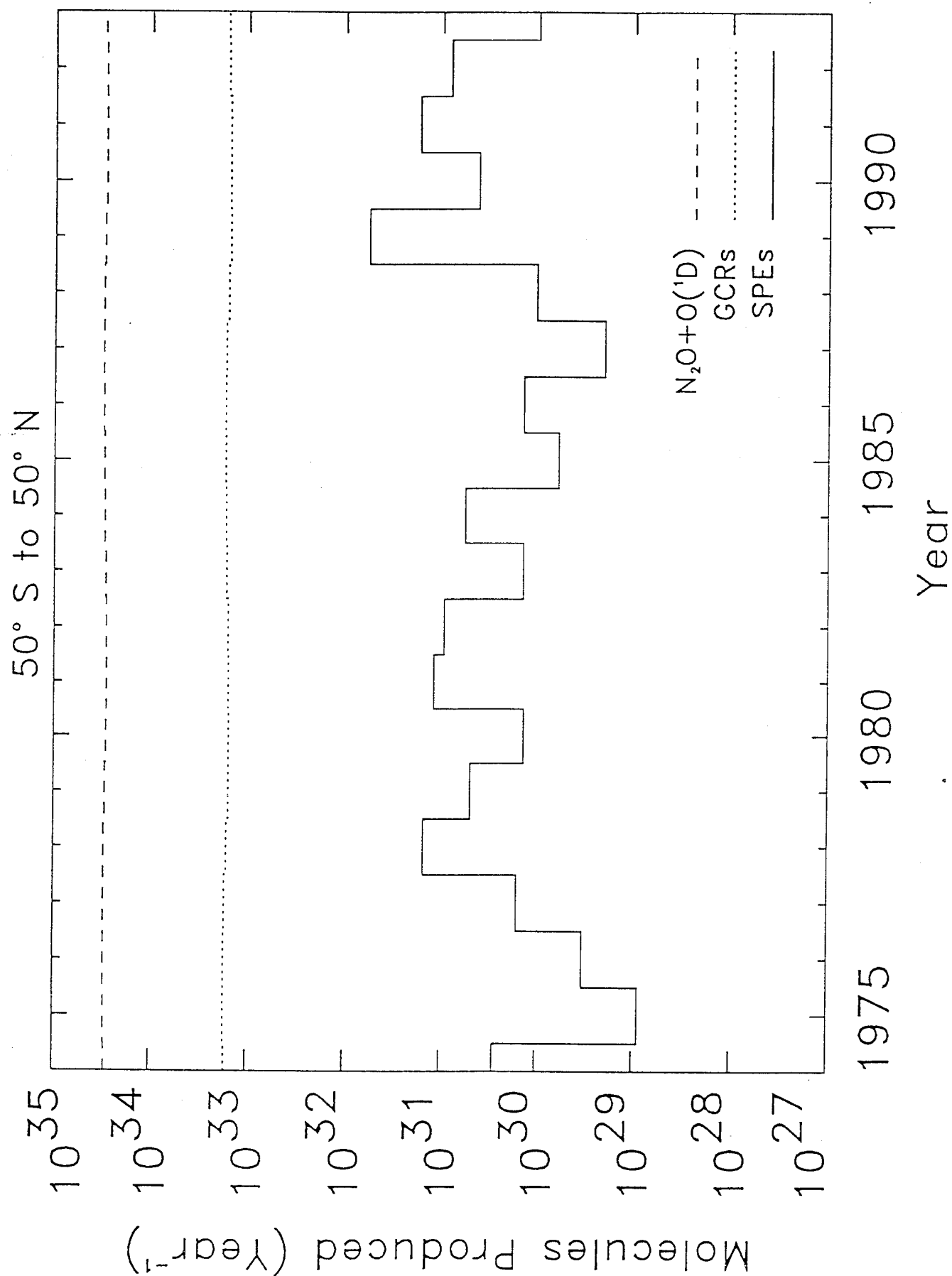


Figure 6

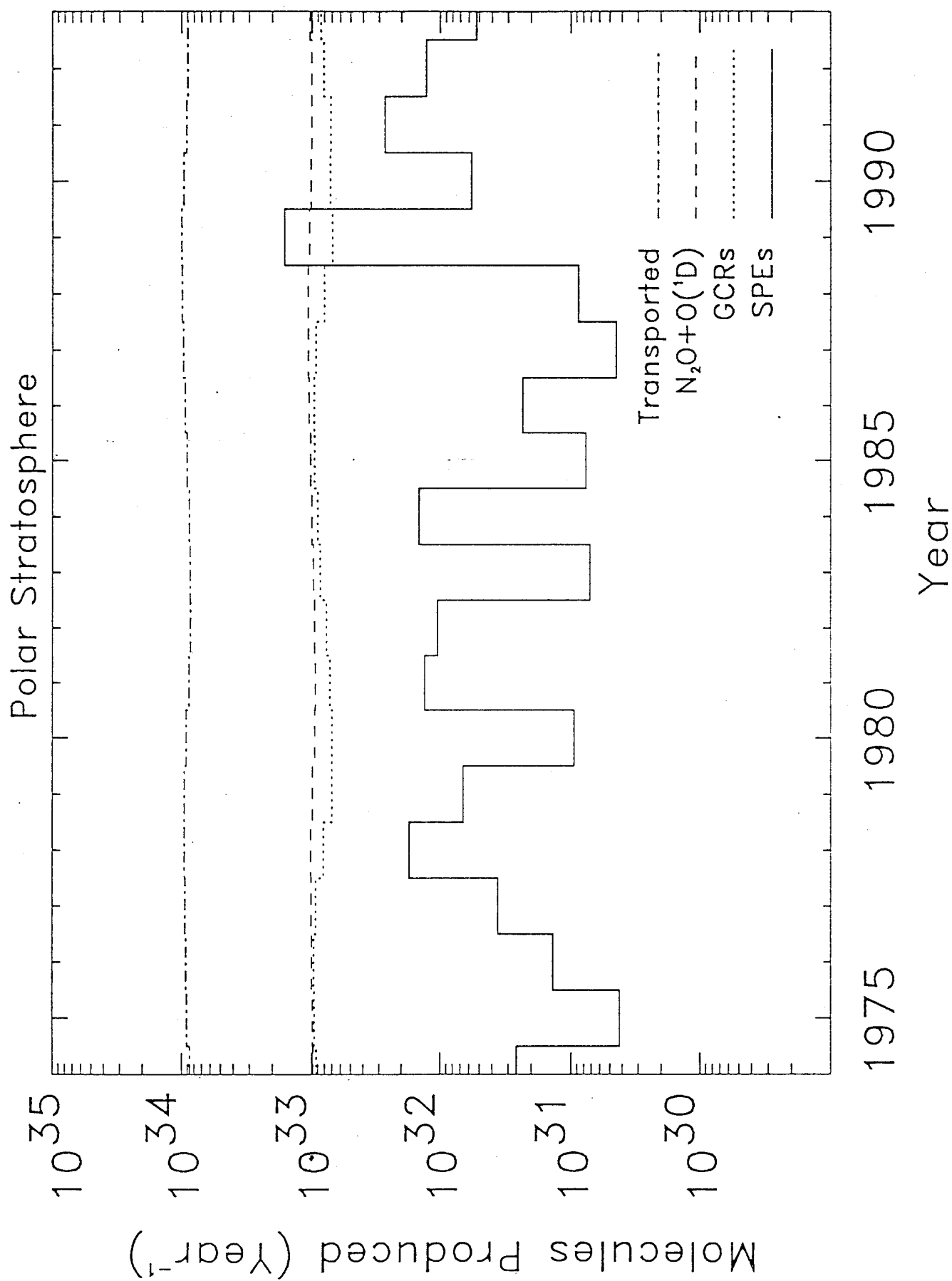


Figure 7